Received: 28 February 2022 | Revised: 03 April 2022 | Accepted: 03 April 2022
DOI: 10.22034/ecc.2022.335453.1394
Eurasian Chemical Communications
SAMI

FULL PAPER

Cancer-curative potential of novel coumarins from watermelon princess: A scenario of their isolation and activity

Reem Nadher Ismael[a,*] | Yasser Fakri Mustafa[a] | Harith Khalid Al-Qazaz[b]

[a]*Department of Pharmaceutical Chemistry, College of Pharmacy, University of Mosul, Mosul, Iraq*
[b]*Department of Clinical Pharmacy, College of Pharmacy, University of Mosul, Mosul, Iraq*

In this research, different types of solvents were used to isolate coumarins from the seeds of Watermelon Princess, including acetone, ether, chloroform, and dichloromethane. Isolation is accomplished by utilizing three approaches: Thermodynamic-, ultrasound-, and microwave-corroborative extractions. These approaches are done in three modalities: non-sequential, sequential rising polarity, and sequential dropping polarity. Based on the findings gathered from the phytoconstituents' assessments, one of the thirty isolates was selected to identify its content of coumarins. Six novel fruit-derived natural coumarins, abbreviated here as **RE1**-**RE6**, have been identified, and their respective molecular backbones are deduced by comparing their spectral data and physical attributes to those previously published. These natural coumarins were tested *in vitro* for two biopotentials. The first is oxidation-protective potential, which was measured by evaluating the ability of our natural coumarins to ambush hydroxyl and DPPH drastic brands. The second is cancer-curative potential, which was investigated via a MTT test against six cancer cell lines. Besides, the undamaging effect of these coumarins on normal cells was investigated using one healthy cell line. From the findings, the authors concluded that product **RE4** could provide a valuable structural template for synthesizing a potent oxidation-protective agent with significant safety. Furthermore, product **RE6** can serve as a foundation stone for the development of potent cancer-curing medications with minimal toxicity to normal tissue.

KEYWORDS

Natural coumarins; phytochemical analysis; antioxidant; anticancer.

***Corresponding Author:**
Reem Nadher Ismael
Email:
reem.20php4@student.uomosul.edu.iq
Tel.: +07730667891

Introduction

Humanity is currently dealing with a slew of medical issues, including microorganisms' and malignant cells' tolerance to currently available medications [1]. To expatiate these issues, medicinal chemists are focusing a lot of their efforts on discovering new natural compounds derived from plants in general and fruits in particular [2,3]. As a result, synthetic chemistry or natural isolation is used in many drug discovery indications [4].

A mismatch between free radical generation and antioxidant protection processes results in oxidative harm which may be implicated in age-related diseases, such as Parkinson's disease and cancer [5,6]. In the literature, many naturally occurring chemicals, including coumarins, stilbenes, lignans, anthocyanins, proanthocyanidins, hydroxycinnamic acids, flavonoids, polyphenols, and others have been shown to provide a natural solution for managing oxidative overload [7,8].

Naturally occurring chemicals and the biological activity associated with them have been a great mystery for several decades for which many researchers are trying to find a solution. Studies of these chemicals are becoming more common in the literature due to the increasing international importance of using these elements to improve human health [9]. More specifically, fruit-derived natural coumarins are playing an important role in identifying unique bioactive template frameworks that may be involved in the process of new medications' development [9,10].

Watermelon Princess waste components are abundant in nutrients since they include a lot of carbs, oils, and amino acids [11]. These waste products also contain many unqualified and quantified secondary metabolic co-products in addition to a variety of helpful cations including calcium, potassium, and magnesium [10,12].

Plant-derived natural coumarins are generally hydrophilic, heterocyclic secondary metabolic co-products. These chemicals can be detected in flowers, leaves, roots, and fruits, among the other different plant parts[13,14]. In hundreds of published books and papers, various biomedical potentials, including anti-pathogenic, anti-diabetic[3,15], anti-oxidant, cancer cell viability inhibition [16], and anti-metabolic syndrome activities of these coumarins have been widely investigated [17,18].

The purposes of this study are to extract natural coumarins from Watermelon Princess seeds and to verify their oxidation-protective and cancer-curative potentials *in vitro*. To achieve this purpose, five targets were considered. First, the acquired crushed powdered seeds were extracted using four various solvents of different polarizations which are acetone, chloroform, dichloromethane, and ether. Three methodologies were utilized for the extraction plan including the thermodynamic-corroborative method (TCM), ultrasound-corroborative method (UCM), and the microwave-corroborative method (MCM). Each utilized method was divided into three modalities, namely non-sequential (NS), sequential rising polarity (SRP), and sequential dropping polarity (SDP). Second, the acquired isolates were assayed for the presence of many primary and secondary metabolic co-products. Third, based on the results of this assay, one isolate was singled out to identify its content of coumarins. Fourth, the structural formulas of the isolated coumarins were established by examining the acquired spectroscopical data and comparing them with those present in the scientific databases. Finally, the *in vitro* bioactivities, including the oxidation-protective and cancer-curative potentials, of the isolated fruit-derived coumarins were evaluated.

Products and procedures

Tokyo Chemical Manufacturing and Sigma-Aldrich supplied the solvents and compounds used in this study. The silica gel (mesh size 100–200, pore size 25Å) was provided by Sisco Research Laboratories Pvt. Ltd.Bio-World provided the MTT dye (Catalog No. 42000092-1) for assaying the cancer-curative potential of the standard drug and the isolated coumarins. The Watermelon Princess batch was purchased from a local vegetable/fruit store and was botanically recognized by experts from Mosul College of Agriculture and Forestry. The separated coumarins' maximum absorption (λ_{max}) wavelength and IR spectra were scanned using two laboratory-grade spectrophotometers. The first named Varian UV/Visible, while the second was Bruker-Alpha ATR. Bruker Analytische Messtechnik GmbH (300 MHz) captured the ^{1}H and ^{13}C-NMR spectra of the separated products using DMSO-d_6 as a solvent [19,20].

Processing of fruit materials

The unique Watermelon Princess from the bought batch (158 kg) was washed properly with tap water, and then distilled water before being hand-sliced into eight slices. The seeds were thoroughly abstracted and dried in a dark environment for two weeks at room temperature before being ground in a spice-grinder and sieved into a very fine powder (266 g). This powder has been stored in airtight amber containers and kept in the refrigerator until ready to use in the advanced stage [21,22].

Extracting process

Ether, dichloromethane, chloroform, and acetone were used as solvents, and three methodologies including TCM, UCM, and MCM were employed in the extraction process. In addition, this process was done in three different modalities: NS, SRP, and SDP. In the SRP model, the sieved powder was extracted using the first solvent (ether) in the polarity trend. Then, the solid was filtered, and the filtrate obtained was assayed for the presence of many primary and secondary metabolic co-products. When the solid is completely dried, it is extracted again with the solvent following the first in the polarity sequence (dichloromethane). In the same fashion, these schematic steps were utilized in the cases of chloroform and acetone solvent types. In the SDP model, the sequence of the schematic steps was also followed but in the reverse order of the solvents employed, i.e., acetone, chloroform, dichloromethane, and then ether [23,24].

Thermodynamic-corroborative method (TCM)

For three days at 30 °C, the seed powder and extractant were mixed at a 10% (w/v%) concentration, and the resultant mixture was thermodynamically agitated. The instrument utilized to perform this agitation type is named SWBR17 SHEL LAB shaking water bath). The resulting sample was filtered and kept in the fridge once it was available, being used to confirm the existence of a variety of primary and secondary metabolic co-products [25,26].

Ultrasound-corroborative method (UCM)

The seed powder and extractant were mixed at a 10% (w/v%) concentration, and the resultant combination was macerated for 30 min at 30 °C. The instrument used to accomplish this type of maceration is named a laboratory grad water bath and is endorsed by an ultrasound generator (40 kHz, 350 W, Power sonic410). The resulting solution was filtered and kept in the fridge once it was willing to be used in the next step of phytochemical screening [27,28].

Microwave-corroborative method (MCM)

The seed powder and extractant were mixed at a 10% (w/v%) concentration, and the resulting mixture was warmed for 5 minutes at 100 W. The appliance employed to provide the energy of extraction is known as a residential convection oven (Moulinex, MW Steam 23L, MW531070). The resulting mixture was filtered and stored in the fridge till it was willing to be used in the next step of phytochemical screening [29].

Primary and secondary metabolic co-products' indicators

Thirty extracts of the previously disclosed extracting process, involving three methodologies and three modalities, were inspected based on the generally recognized procedures given by Harborne [30–32] for the presence of different primary and secondary co-products. These co-products include glycosides, saponins, steroids, flavonoids, amino acids, proteins, phenols, anthocyanins, emodins, fixed oils, alkaloids,

carbohydrates, terpenoids, tannins, and coumarins.

Separation and isolation

Depending on the outcomes indicated in Tables 1-3, a chloroform extract of an SRP modality achieved from the UCM was preferred to distinguish its coumarin content. The procedure began with macerating 200 grams of ground seed powder into 2L of extractant. After the extraction, the crude (15.02 g) was unsettled for 15 min at 50°C in 150 mL of 1 M NaOH without first being filtered. Drop by drop, 1 M HCl was added to the pale yellow filtrate in a chilled bucket, and the handling was discharged when the solution color disappeared completely. To complete the process of crystal formation, the mixture was preserved in the fridge for one day, after which it was filtered and balanced (111.4 g) [33].

The elevated TLC model was used to identify how many coumarin-based products may present in the isolate. A spot on the TLC plate was invented by solubilizing a small amount of crystals in 2 mL of chloroform. A 4:1 mixture of chloroform and acetone was used as an eluting system, and the isolated dots were localized using UV light advice set at specific wavelength (366 nm). Six spots were discovered in the triplicate results. To isolate the coumarin-based products, column chromatography was used with ether: ethyl acetate solutions in curve ratios ranging from 1:9 to 9:1 as the separating system and silica gel as the solid system. **RE1**-**RE6** is six new simple coumarins discovered in different eluent systems with such specific TLC plate locations [33].

Evaluation of the oxidation-protective potential

The capacity of the extracted natural coumarins (ENCs) to ambush DPPH (1,1-diphenyl-2-picryl-hydrazyl) and hydroxyl drastic brands, as well as play a role in an oxidation-reduction reaction, was measured using a regulate, which was a solution of typical antioxidant L-ascorbic acid (L-AA). Various diluted quantities of the experimented coumarins were used including 200, 100, 50, 25, 12.5, and 6.25 µM employing the principal liquid medium as a diluent. Depending on the following mathematical formula, the scores of ambushing percent (A%) for the applied concentrations were calculated regarding each product:

$$\boldsymbol{A}(\%) = \boldsymbol{Ab_c} - \boldsymbol{Ab_t} \div \boldsymbol{Ab_c} \times \mathbf{100}$$

The acronyms "Ab_c" and "Ab_t" refer to the evaluated absorption bands of regulate and experimented samples at different colored wavelengths. A non-linear statistical graph depicting the relationship between A% and the log concentration of the regulate or experimented coumarin was used to calculate the ambush activity denoted as AA_{50}, the concentration of the specimen required to ambush 50% of the drastic brands [34,35].

Ambushing activity versus DPPH drastic brands

An ethanolic solution (1.5 mL) of regulate or experimented coumarin was mixed with an ethanolic DPPH solution at a given concentration (0.5 mL, 0.1 mM). The mixed solution was overlaid with aluminum plates to hide it from daylight, and the coated solution was kept at 25°C for 30 min. At 517 nm, the ability of the experimented coumarin to ambush DPPH drastic brands was measured by the colorimetric methodology. The surveillance solution consisted of 1.5 mL of ethanol and 0.5 mL of ethanolic DPPH solution [34,36].

Ambushing activity versus hydroxyl drastic brands

A pre-determined concentration of regulate or experimented coumarin (1.5 mL) was mixed with 2.4 mL of phosphate-buffered

saline (0.2M, pH 7.8). Thereafter, the resultant reaction was amplified by adding three promoters, including ferric chloride, pyridino[3,2-h]quinolone, and hydrogen dioxide in the following volumes: 60 µL (0.001 M) ferric chloride, 90 µL (0.001 M), and 150 µL (0.17 M), respectively. The resultant solution was incubated at 25°C for 5 min before being analyzed by the colorimetric methodology at 560 nm. The surveillance solution contains all of the aforementioned components, however, the regulate or experimented coumarin has been replaced by phosphate-buffered saline [37].

Cancer-curative potential

ENCs were tested for cancer-curative potential versus six experimental tumor types, namely KYSE-30, SK-OV-3, AMN3, SKG, HeLa, and MCF-7. The full descriptions of these cell lines are Human Asian Esophageal Squamous Cell Carcinoma, Caucasian Ovary Adenocarcinoma, Murine Mammary Adenocarcinoma, Human Papillomavirus-Related Cervical Squamous Cell Carcinoma, Epithelioid Cervix Carcinoma, and Caucasian Breast Adenocarcinoma, respectively. Likewise, the global codes of these tumor lines are 94072011, 91091004, CVCL-M395, C27676, 93021013, and 86012803, respectively.

Cell vitality can be determined using the MTT (3-[4, 5-dimethylthiazol-2-yl]-2,5diphenyl tetrazolium bromide) methodology. The ENCs, as well as the well-recognized anti-proliferative medication 5-fluoruracil (5F-uracil), are being serially diluted by DMSO at five different doses (200, 100,50,25,12.5, and 6.25 µM).

After one day, the experimental cancerous cell lines were divided into 10,000 cells per well in a 96-well plate and treated independently with varying doses of 5F-uracil or the experimental coumarins. The vitality of the cells was determined after three days of treatment in three sequential steps. The vitality of the cells was determined after three days of treatment in three sequential steps. First, the nutrient-containing medium was eliminated. Second, the visual marker, MTT, solution 28 µL, 3.27 mM was included, and finally, the marked and unmarked cells were incubated at 37 °C for 90 min [38,39].

A microtiter plate viewer established at 492 nm was used to quantify the absorbance values of the treated and untreated wells (Abt and Abu). The percentage of growth suppression was calculated using the simple mathematical methodology below. The IC_{50}, or the intensity of the specimen demanded to disestablish 50% of the cellular growth was calculated using a quasi-statistical diagram featuring the correlation between both the growth suppression percent and the log intensity of the regulate or experimented coumarin [40].

$$Growth\ suppression\ (\%) = \frac{Abt - Abu}{Abt} \times 100$$

Results and discussion

In the past two decades, many medical academics have recommended the utilization of naturally occurring products as popular remedies for managing several illnesses. In addition to their safe utilization for a long time, naturally occurring products are considered a remarkable source of bioactive scaffolds. These bioactive templates offer a lot of stimulation towards the translation of their molecular backbones into medically valuable remedies [40].

Plant-based medications are much more available, less expensive, safer, and efficacious, with fewer side effects generally [10].

Separation and structural characterization of secondary metabolic co-products are two of the major challenges facing researchers in the field of naturalist origin products. These difficulties were exacerbated by the effort to combine the existence of specific structural

traits with the diverse biological actions of separated products [40].

Bibliography of primary and secondary metabolic co-products

The results gathered from various employed inspection indicators draw a detailed map of the primary and secondary metabolic co-products in the Watermelon Princess seeds. From the careful observation of this map, the authors chose the chloroform extract of a SRP modality obtained from the UCM to isolate its content of coumarins. This recommendation was based on the fact that this isolate is free from "flavonoids", "alkaloids", "tannins", and "fixed oils", where their presence may interfere with the separation chemical base. Tables 1-3 display the names of co-products and their corresponding inspection indicators, as well as the observed outcomes from conducting these markers.

TABLE 1 The names of co-products and their corresponding inspection indicators, as well as the outcomes observed from applying these tests using TCM in NS, SRP, and SDP modalities

Names of co-products	Inspection indicators	Acetone		Chloroform			Dichloromethane			Ether	
		NS	SRP	NS	SRP	SDP	NS	SRP	SDP	NS	SDP
Flavonoid (s)	Pews indicator	×	×	×	×	×	×	×	×	×	×
	Lead acetate indicator	×	√	√	×	×	√	×	×	×	×
Tannin (s)	Braymer's indicator	√	√	×	×	×	×	×	×	×	×
Carbo-hydrate (s)	Molisch's indicator	√	√	×	√	√	√	√	×	√	×
Phenol (s)	Ferric chloride indicator	×	×	×	×	×	×	×	×	×	×
Terpenoid (s)	Libermann-Burchard indicator	√	√	√	×	√	√	×	×	√	×
Emodin (s)	Ammonium hydroxide indicator	×	×	×	×	×	×	×	×	×	×
Steroid (s)	Salkowski indicator	√	√	√	√	√	√	×	√	√	×
Glycoside (s)	Liebermann's indicator	×	×	×	×	×	×	×	×	×	×
Protein (s)	Xanthoproteic indicator	×	√	√	√	√	×	√	√	√	√
Amino- acid (s)	Ninhydrin indicator	×	√	√	√	√	×	√	√	√	√
Alkaloid (s)	Mayer's indicator	√	×	√	√	√	√	×	√	×	×
Betacyanin (s)	Pigment-dependent indicator	√	√	√	×	√	√	×	√	√	√
Antho-cyanin (s)		×	×	×	×	×	×	×	×	×	×
Saponin (s)	Foam indicator	×	×	×	√	√	√	√	×	×	×
	Olive oil indicator	×	×	×	×	×	×	×	×	×	×
Anthra-quinone (s)	Borntrager's indicator	×	×	×	×	×	×	×	×	×	×
Fixed-oil (s)	spot indicator	√	×	√	×	×	√	×	×	√	×
	Saponification indicator	×	×	×	√	√	×	×	√	×	×
Coumarin (s)	NaOH indicator	√	√	√	√	√	√	√	√	√	√
	Fluorescence indicator	√	√	√	√	√	√	√	√	√	√

TABLE 2 The names of co-products and their corresponding inspection indicators, as well as the outcomes observed from applying these tests using UCM in NS, SRP, and SDP modalities

Names of co-products	Inspection indicators	Acetone		Chloroform			Dichloromethane			Ether	
		NS	SRP	NS	SRP	SDP	NS	SRP	SDP	NS	SDP
Flavonoid (s)	Pews indicator	×	×	×	×	×	×	×	×	×	×
	Lead acetate indicator	√	×	×	×	×	√	√	×	×	×
Tannin (s)	Braymer's indicator	√	√	×	×	×	×	×	×	√	√
Carbo-hydrate (s)	Molisch's indicator	×	√	√	×	√	√	×	√	√	√
Phenol (s)	Ferric chloride indicator	×	×	×	×	×	×	×	×	×	×
Terpenoid (s)	Libermann-Burchard indicator	√	√	×	×	√	√	×	×	√	×
Emodin (s)	Ammonium	×	×	×	×	×	×	×	×	×	×

	hydroxide indicator										
Steroid (s)	Salkowski indicator	×	×	×	√	√	√	√	√	√	√
Glycoside (s)	Liebermann's indicator	×	×	×	×	√	×	√	×	×	×
Protein (s)	Xanthoproteic indicator	×	×	√	√	√	√	√	√	√	√
Amino- acid (s)	Ninhydrin indicator	×	×	√	√	√	√	√	√	√	√
Alkaloid (s)	Mayer's indicator	√	×	√	×	√	√	√	×	√	√
Betacyanin (s)	Pigment-dependent indicator	√	√	√	×	√	√	√	√	×	×
Antho-cyanin (s)		×	×	×	×	×	×	×	×	×	×
Saponin (s)	Foam indicator	√	×	√	×	√	√	×	√	×	×
	Olive oil indicator	×	√	×	×	×	√	×	√	×	×
Anthra-quinone (s)	Borntrager's indicator	×	×	×	×	√	×	×	×	×	×
Fixed-oil (s)	spot indicator	√	×	√	×	√	×	×	×	√	×
	Saponification indicator	×	√	×	×	×	×	×	×	√	×
Coumarin (s)	NaOH indicator	√	√	√	√	√	√	√	√	√	√
	Fluorescence indicator	√	√	√	√	√	√	√	√	√	√

TABLE 3 The names of co-products and their corresponding inspection indicators, as well as the outcomes observed from applying these tests using MCM in NS, SRP, and SDP modalities

Names of co-products	Inspection indicators	Acetone		Chloroform			Dichloromethane			Ether	
		NS	SRP	NS	SRP	SDP	NS	SRP	SDP	NS	SDP
Flavonoid (s)	Pews indicator	×	×	×	×	×	×	×	×	×	×
	Lead acetate indicator	×	√	√	×	√	√	×	×	×	×
Tannin (s)	Braymer's indicator	√	√	×	×	×	×	×	×	×	×
Carbo-hydrate (s)	Molisch's indicator	√	√	√	√	×	×	×	×	√	√
Phenol (s)	Ferric chloride indicator	√	√	×	×	×	×	×	×	×	×
Terpenoid (s)	Libermann-Burchard indicator	√	√	√	√	√	√	√	√	√	√
Emodin (s)	Ammonium hydroxide indicator	×	×	×	×	×	×	×	×	×	×
Steroid (s)	Salkowski indicator	√	√	√	√	√	√	√	√	√	×
Glycoside (s)	Liebermann's indicator	×	×	×	×	×	×	×	×	×	×
Protein (s)	Xanthoproteic indicator	×	×	√	√	√	√	√	√	√	√
Amino- acid (s)	Ninhydrin indicator	×	×	√	√	√	√	√	√	√	√
Alkaloid (s)	Mayer's indicator	×	×	×	×	×	×	×	×	×	×
Betacyanin (s)	Pigment-dependent indicator	×	√	√	√	√	√	√	√	√	×
Antho-cyanin (s)		×	×	×	×	×	×	×	×	×	×
Saponin (s)	Foam indicator	×	×	√	√	√	√	√	√	×	×
	Olive oil indicator	×	×	×	×	×	√	√	√	√	√
Anthra-quinone (s)	Borntrager's indicator	×	×	×	×	×	×	×	×	×	×
Fixed-oil (s)	spot indicator	×	×	×	×	×	×	×	×	×	×
	Saponification indicator	√	×	√	√	√	√	×	×	√	×
Coumarin (s)	NaOH indicator	√	√	√	√	√	×	√	√	√	√
	Fluorescence indicator	√	√	√	√	√	×	√	√	√	√

Note: In the previous tables, the acronyms √ and × relate to the positives and negatives for three trials, respectively

Separation and isolation

When coumarins are threatened by an influential nucleophile like NaOH, the cyclic ester (lactone) is catabolized into hydrophilic salts of cis-cinnamic acid as a by-product. Whenever these salts are acidified, the native coumarins are repaired, as depicted in Figure 1. This catabolizing-anabolizing turn-on/off was used as a principle for isolating Watermelon Princess-derived coumarins in the present study [23].

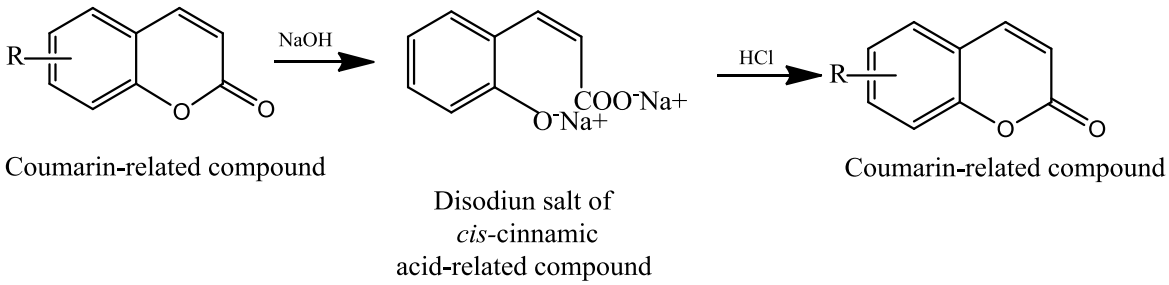

FIGURE 1 The catabolizing-anabolizing turn-on/off method utilized in the isolation process

Characterization of the RE1-RE6 chemical structures

Analyzing the physical attributes and spectroscopic data of the Watermelon Princess-derived coumarins, as well as comparing these attributes and data with those found in the published works, provided the basis for the characterization of these coumarins. As a result, the authors concluded that the Watermelon Princess-derived coumarins shared the presence of a coumarin core functionalized with a hydroxyl group at position 7. This shared structure is commonly known as an umbelliferon. Accordingly, the Watermelon Princess-derived coumarins **RE1-RE6**, as shown in Figure 2, can be classified as novel simple coumarins with chemical structures based on umbelliferon [14].

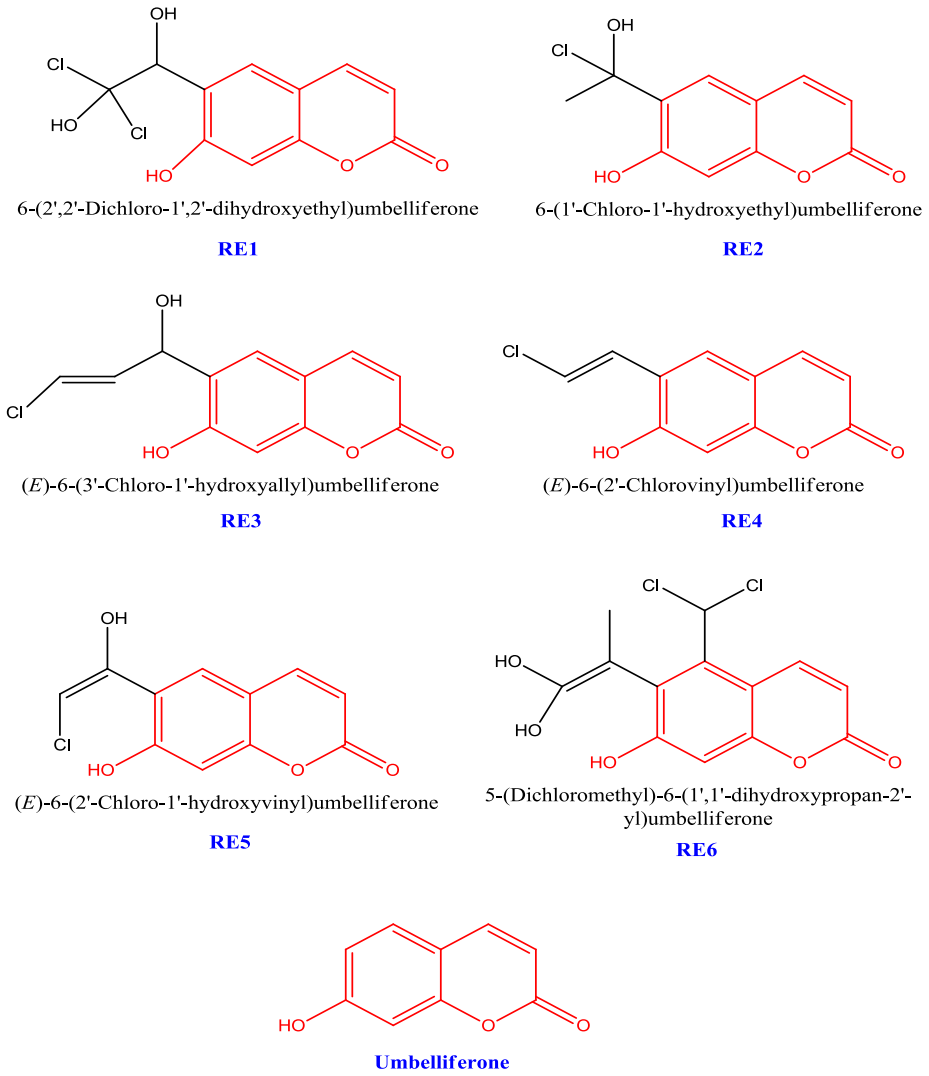

FIGURE 2 The chemical structures of the Watermelon Princess-derived coumarins, **RE1-RE6**, and their precursor umbelliferone

The spectroscopic data of RE1-RE6 and Their physical attributes

6-(2',2'-Dichloro-1',2'-dihydroxyethyl)umbelliferone (**RE1**): Off-white powder; Mobile phase (ether: ethyl acetate 4.5:5.5); Weight (119.78 µg/g of dried seeds' powder); mp 160-162 °C; R_f 0.53; UV (EtOH) λ_{max} 401 nm; IR ν_{max} 3473 (broad, alcoholic OH str.), 3404 (broad, phenolic OH str.), 3062 (weak, alkene C-H str.), 2895 (weak, saturated alkyl C-H str.), 1735 (strong, cyclic ester of lactone C=O str.), 1592 (strong, *cis* C=C str.), 1551 (medium, aryl conjugated double bond of C=C str.), 733 (strong, aliphatic C-Cl) cm^{-1}; ^{1}H-NMR (DMSO-d_6, 300 MHz): δ=3.78 (1H, s, OH-2'), 3.85 (1H, s, OH-1'), 5.34 (1H, s, H-1'), 5.73 (1H, s, OH-7), 6.23 (1H, d, *J*=9 Hz, H-3), 6,92 (1H, s, H-8), 7,72 (1H, d, *J*=9 Hz, H-4), and 8.11 (1H, s, H-5) ppm; ^{13}C-NMR (DMSO-d_6, 75 MHz): δ=89.5 (CH, C-1'), 107.9 (CH, C-8), 115.4 (CH, C-3), 117.7 (CH, C-10), 125.2 (C, C-2'), 127,1 (CH, C-6), 131.4 (CH, C-5), 143.7 (CH, C-4), 155.4 (C, C-7), 158.0 (C, C-9), and 162.2 (C, C-2) ppm.

6-(1'-Chloro-1'-hydroxyethyl) umbelliferone (**RE2**): Whitish powder; Mobile phase (ether: ethyl acetate 5.5:4.5); Weight (108.21 µg/g of dried seeds' powder); mp 148-150 °C; R_f 0.59; UV (EtOH) λ_{max} 384 nm; IR ν_{max} 3473 (broad, alcoholic OH str.), 3404 (broad, phenolic OH str.), 3062 (weak,

alkene C-H str.), 2896 (weak, saturated alkyl C-H str.), 1734 (strong, cyclic ester of lactone C=O str.), 1592 (strong, *cis* C=C str.), 1551 (medium, aryl conjugated double bond of C=C str.), 735 (strong, aliphatic C-Cl) cm^{-1}; ^{1}H-NMR (DMSO-d_6, 300 MHz): δ= 2.04 (3H, s, H-2'), 3.84 (1H, s, OH- 1'), 5.73 (1H, s, OH-7), 6.23 (1H, d, *J*=9 Hz, H-3), 6.92 (1H, s, H-8), 7.72 (1H, d, *J*=9 Hz, H-4), and 8.12 (1H, s, H-5) ppm; ^{13}C-NMR (DMSO-d_6, 75 MHz): δ=33.2 (CH_3, C-2'), 95.0 (CH, C-1'), 107.8 (CH, C-8), 115.4 (CH, C-3), 117.8 (C, C-10), 123.6 (C, C-6), 131.3 (CH, C-5), 143.7 (CH, C-4), 157.3 (C, C-7), 158.1 (C, C-9), and 162.2 (C, C-2) ppm.

(*E*)-6-(3'-Chloro-1'-hydroxyallyl) umbelliferone (**RE3**): Pale yellow powder; Mobile phase (ether: ethyl acetate 8:2); Weight (91.04µg/g of dried seeds' powder); mp 185-187°C; R_f 0.71; UV (EtOH) λ_{max} 466 nm; IR v_{max}3347 (broad, alcoholic OH str.), 3383 (broad, phenolic OH str.), 3072 (weak, *cis* alkene C-H str.), 3039 (weak, *trans* alkene C-H str.), 1735 (strong, cyclic ester of lactone C=O str.), 1637 (strong, *trans* C=C str.), 1589 (medium, *cis* C=C str.), 1553 (m, aryl conjugated double bond of C=C str.), 733 (strong, aliphatic C-Cl) cm^{-1}; ^{1}H-NMR (DMSO-d_6, 300 MHz): δ=3.92 (1H, s, OH-1'), 5.42 (1H, s, H-1'), 5.68 (1H, s, , OH-7), 6.30 (1H, d, *J*=9 Hz, H-3), 6.58 (1H, d, *J*=15, H-3'), 6.78 (CH, d, *J*=15, H-2'), 7.00 (1H, s, H-5), 7.10 (1H, s, H-8), and 8.17 (1H, d, *J*=9 Hz, H-4) ppm; ^{13}C-NMR (DMSO-d_6, 75 MHz): δ=64.2 (CH_3, C-1'), 110.2 (CH, C-8), 133.8 (CH, C-3), 114.6 (C, C-10), 115.4 (CH, C-3'), 124.3 (C, C-6), 126.4 (CH, C-5), 130.2 (CH, C-2'), 143.7 (CH, C-4), 154.4 (C, C-7), 157.1 (C, C-9), and 160.8 (C, C-2) ppm.

(*E*)-6-(2'-Chlorovinyl)umbelliferone (**RE4**): Yellowish powder; Mobile phase (ether: ethyl acetate 8.5:1.5); Weight (88.14 µg/g of dried seeds' powder); mp 199-201 °C; R_f 0.78; UV (EtOH) λ_{max} 502 nm; IR v_{max}3386 (broad, phenolic OH str.), 3073 (weak, *cis* alkene C-H str.), 3037 (weak, *trans* alkene C-H str.), 1735 (strong, cyclic ester of lactone C=O str.), 1636 (weak, *trans* C=C str.), 1592 (weak, cis C=C str.), 1550 (medium, aryl conjugated double bond of C=C str.), 735 (strong, aliphatic C-Cl) cm^{-1}; ^{1}H-NMR (DMSO-d_6, 300 MHz): δ=5.68 (1H, s, OH-7), 6.31 (1H, d, *J*=9 Hz, H-3), 6.97 (1H, s, H-5), 7.12 (1H, s, H-8), 7.30 (1H, d, *J*=15 Hz, H-2'), 7.51 (1H, d, *J*=15 Hz, H-1'), and 8.17 (1H, d, *J*=9 Hz, H-4) ppm; ^{13}C-NMR (DMSO-d_6, 75 MHz): δ=109.3 (C, C-6), 110.6 (CH, C-8), 111.2 (C, C-10), 113.8 (CH, C-3), 114.9 (CH, C-2'), 119.3 (CH, C-5), 128.4 (CH, C-1'), 143.7 (CH, C-4), 155.0 (C, C-7), 157.4 (C, C-9), and 160.8 (C, C-2), ppm.

(*E*)-6-(2'-Chloro-1'-hydroxyvinyl) umbelliferone (**RE5**): Light yellow powder; Mobile phase (ether: ethyl acetate 6.5:3.5); Weight (80.65 µg/g of dried seeds' powder); mp 212-214 °C; R_f 0.66; UV (EtOH) λ_{max} 489 nm; IR v_{max} 3473 (broad, alcoholic OH str.), 3382 (broad, phenolic OH str.), 3085 (weak, *cis* alkene C-H str.), 3056 (weak, *trans* alkene C-H str.), 1732 (strong, cyclic ester of lactone C=O str.), 1671(weak, *trans* C=C str.), 1626, 1589 (weak, *cis* C=C str.), 1555 (medium, aryl conjugated double bond of C=C str.), 736 (strong, aliphatic C-Cl) cm^{-1}; ^{1}H-NMR (DMSO-d_6, 300 MHz): δ=5.67 (1H, s, OH-7), 6.56 (1H, d, *J*=9 Hz, H-3), 6.93 (1H, s, H-5), 7.03 (1H, s, H-8), 7.19 (1H, s, H-2'), 8.35 (1H, d, *J*=9 Hz, H-4), and 12.05 (1H, s, OH-1') ppm; ^{13}C-NMR (DMSO-d_6, 75 MHz): δ=79.7 (CH, C-2'), 104,5 (C-C, C-6), 110.6 (CH, C-8), 111.2 (C, C-10), 113.8 (CH, C-3), 119.3 (CH, C-5), 143.7 (CH, C-4), 155.7 (C, C-7), 157.4 (C, C-9), 160.8 (C, C-2), and 181.1 (C, C-1') ppm.

5-(Dichloromethyl)-6-(1',1'-dihydroxypropan-2'-yl) umbelliferone (**RE6**): Pale yellow powder; Mobile phase (ether: ethyl acetate 3.5:6.5); Weight (69.11µg/g of dried seeds' powder); mp 170-172 °C; R_f 0.44; UV (EtOH) λ_{max} 453 nm; IR v_{max} 3474 broad, alcoholic OH str.), 3402 (broad, phenolic OH str.), 3060 (weak, alkene C-H str.), 2872 (weak, saturated alkyl C-H str.), 1733 (strong, cyclic ester of lactone C=O str.), 1591 (weak, *cis* C=C str.), 1551 (medium, aryl conjugated double bond of C=C str.), 734 (strong, aliphatic C-Cl) cm^{-1}; ^{1}H-NMR (DMSO-d_6, 300 MHz): δ=2.82 (3H, s, CH3-1'), 5.70 (1H, s, OH-

7), 6.24 (1H, d, *J*=9 Hz, H-3), 6.92 (1H, s, H-8), 7.31 (1H, s, $CHCl_2$-5), 7.74 (1H, d, *J*=9 Hz, H-4), and 12.2 (2H, s, OH-2') ppm; ^{13}C-NMR (DMSO-d_6, 75 MHz): δ=21.1 (CH_3, CH_3 -1'), 70.6 (CH, $CHCl_2$-5), 78.2 (C, C-1'), 109.5 (CH, C-8), 115.4 (CH, C-3), 121.4 (C, C-10), 122.3 (C, C-6), 140.4 (C, C-5), 141.2 (CH, C-4), 157.5 (C, C-9), 160.2 (C, C-7), 162.2 (C,C-2), and 206.4 (C, C-2') ppm.

Oxidation-protective activity

The antioxidant study has sparked renewed attention in recent years, primarily for its possible involvement in the care and mitigation of a variety of disorders that influence human health, including diabetes, cancer, and Alzheimer's disease. The discovery of novel antioxidants obtained from nature has piqued people's attention in a big way. In this respect, a link has been established between the structural properties of ENCs and their oxidation-protective ability, which has been widely identified in this study. The number of OH-groups connected to the aromatic region of the coumarin core may affect this ability, as well as the capacity of the ortho substitution (s) to the OH-group to donate electrons [11]. This association was matched and parallel to those findings recorded in Table 4 and illustrated as a diagram in Figure 3. The ENCs are shown to have DPPH ambushing potential in the following order: **RE2**, **RE4**, **RE6**, **RE3**, **RE5**, **and RE1**. Product **RE2**, which has one alcoholic-OH and one phenolic-OH with less steric hindrance, showed a bitter ability to ambush DPPH drastic brands than the other ENCs. Although compound **RE1** has two alcoholic-OH groups in addition to one phenolic-OH group, it demonstrated the least activity because of the OH-groups' greater steric hindrance.

Regarding the ambushing effect versus hydroxyl drastic brands, the ENCs are shown to have this effect in the following order: **RE4**, **RE3**, **RE2**, **RE6**, **RE1**, and **RE5**. Product **RE4** exhibits the best capacity, while product **RE5** exhibits the least ability due to the H-bond discovered between the OH-group and the 2' chloride accredited highly conjugated system capable of quenching OH-radicals. This portion has a detrimental influence on **RE5** since the enolic OH-group gives large electrons to chloride atoms which are attached to carbon number 2, limiting the conjugated system.

TABLE 4 The results of the regulate and experimented coumarins regarding their oxidation-protective activity

Derivative symbol		DPPH-radical ambushing effect AA_{50} (μM) ±SD		Hydroxyl-radical ambushing effect AA_{50} (μM) ±SD	
	L-AA		46.11±1.40		50.27±0.95
	RE1		103.09±1.09		65.74±1.17
	RE2		56.23±0.97		64.07±1.07
	RE3		61.76±0.97		62.55±1.04
	RE4		56.81±1.05		61.24±1.03
	RE5		64.07±0.99		66.28±1.03
	RE6		58.91±0.98		64.32±1.06

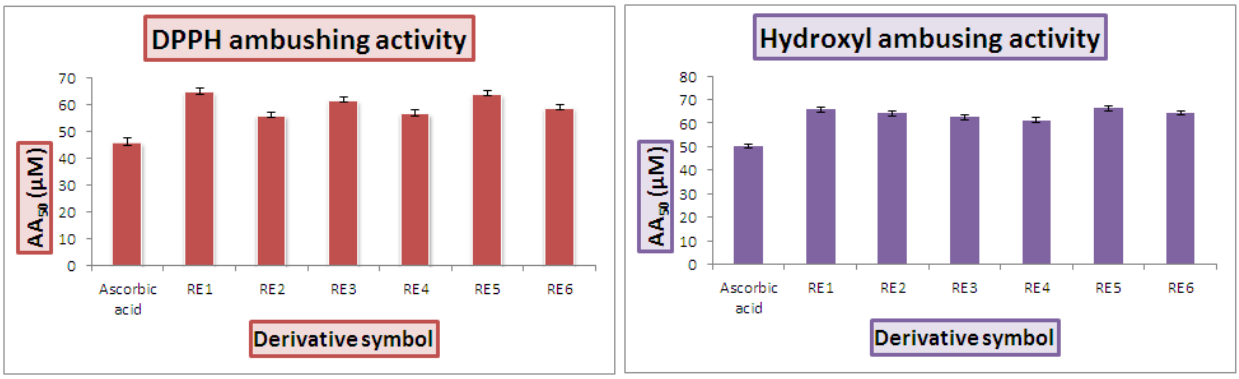

FIGURE 3 Visually representation of the results acquired from investigating the ambushing effect versus DPPH and hydroxyl drastic brands

Cancer-curative activity

By using MTT marking dye, the cancer-curative activity of the ENCs was investigated versus six malignant cell lines, included KYSE-30, SK-OV-3, AMN3, SKG, HeLa, and MCF-7. Moreover, the undamaging effect of our coumarins on normal cell line named RWPE-1 was inspected.

The authors concluded several definitive points when analyzing the data recorded in Table 5 and graphically illustrated in Figures 4 and 5. First, when compared to the tested malignant cell lines, the experimental coumarins demonstrated a similar trend of cancer-curative activity. The trend of this activity is **RE6**, **RE4**, **RE2**, **RE1**, **RE5**, and **RE3**. Second, these coumarins had a similar trend of undamaging effect on the normal cell line, which is in contrast to that reported in the cancer-curative activity. The order of this effect is **RE3**, **RE5**, **RE1**, **RE2**, **RE4**, and **RE6**.

Third, the coumarins had significant cancer-curative activity compared with 5F-uracil, with a privilege potency contributed to **RE6** and then to **RE4**. The authors proposed that this potency may be due to the number of Cl-groups and their rotation-free state. Product **RE6** includes two Cl-groups (5-dichloromethyl) that may spin freely and organize in many orientations, enabling the interaction with the target protein's binding site in various ways. Product **RE1**, which is located at the midpoint of the trend, contains two Cl-groups (at carbon 2') that are enclitic with two alcoholic OH-groups, resulting in the formation of two H-bonds, which may contribute to restricting the free rotation of Cl-groups and making them unavailable to form interactions with the target protein's binding site, lowering cell viability inhibitory effect. Product **RE3**, which has the lowest activity, contains one Cl-group with restricted motion because of the double bond. Also, this group is surrounded by phenolic-OH and enolic-OH with a high probability of hydrogen bond formation.

Fourth, the influence of the Cl-groups and their rotation-free state play an opposite impact on the undamaging effect of our coumarins. Finally, compared with 5F-uracil and the other Watermelon Princess derived coumarins, **RE6** has the best cancer-curing activity versus the involved malignant cell lines and the highest undamaging effect on the normal cell line.

TABLE 5 The acquired results from examining the cancer-curative activity versus malignant cell lines and the undamaging effect on normal cell line

Symbol	MCF-7 Cancer cell line		HeLa Cancer cell line		SKG Cancer cell line		AMN3 Cancer cell line		SK-OV-3 Cancer cell line		KYSE-30 Cancer cell line		RWPE-1 Cancer cell line	
5F-uracil	**TC50**	**SD**	**TC50**	**SD**	**TC50**	**SD**	**TC50**	**SD**	**TC50**	**SD**	**TC50**	**SD**	**TC50**	**SD**
RE1	12.39	0.93	13.23	0.97	22.1	1.01	24.71	1.03	22.16	1.02	30.33	0.99	34.35	0.98
RE2	22.75	1.06	16.04	1.08	35.87	1.03	26.24	1.01	27.96	0.98	41.28	1.11	327.87	1.00
RE3	15.58	0.92	15.13	0.98	34.41	1.04	26.43	1.00	27.23	0.95	41.26	0.98	331.84	0.96
RE4	30.78	1.00	22.01	1.07	35.94	0.99	32.30	1.03	39.21	1.00	45.42	1.01	321.87	0.99
RE5	14.42	0.96	14.32	1.02	31.69	1.01	26.84	0.99	24.36	1.01	36.85	0.97	336.02	0.97
RE6	26.81	0.99	18.24	1.04	34.64	1.11	34.49	1.05	31.29	0.98	47.33	1.01	325.95	0.97
	13.96	1.11	13.65	1.12	28.73	0.99	24.68	1.06	24.37	0.97	28.54	1.06	658.54	1.03

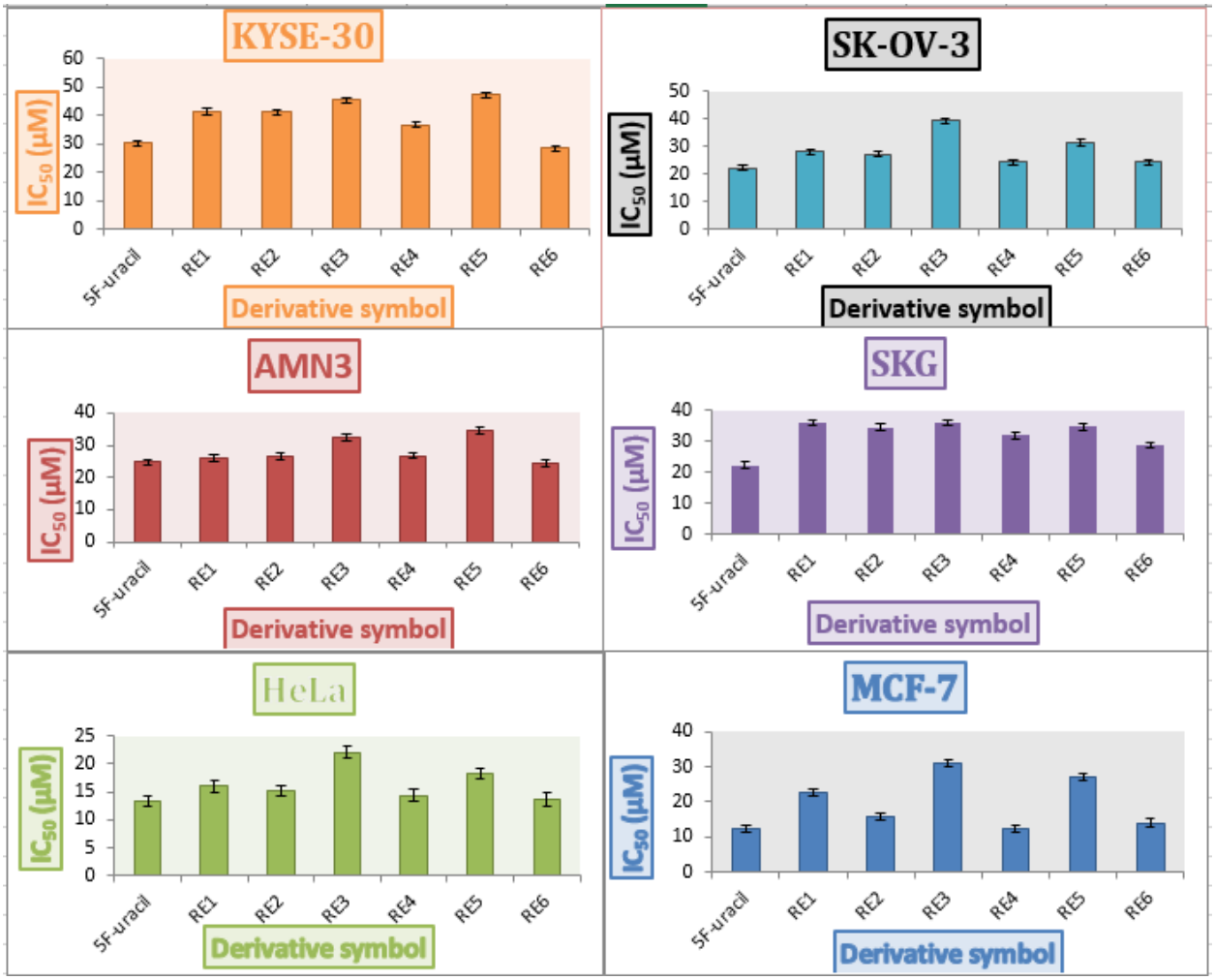

FIGURE 4 Visually representation of the results acquired from investigating the cancer-curative activity of ENCs versus different malignant cell lines

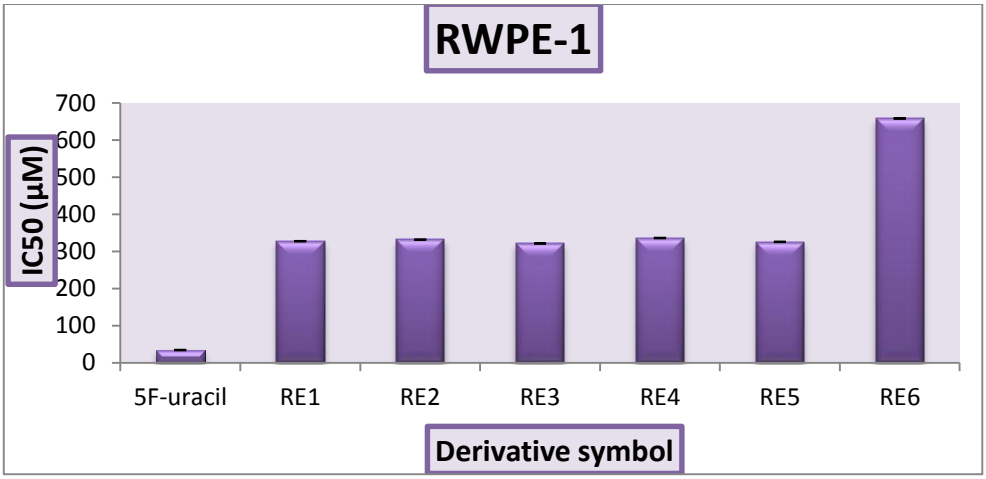

FIGURE 5 Visually representation of the results acquired from investigating the undamaging effect of ENCs on normal cell line

Conclusion

This study described the isolation and characterization of six new fruit-derived, naturally occurring coumarins with their unique umbelliferone cores isolated from Watermelon Princess crushed seed powder. ENCs have been found to have potent-to-moderate oxidation-protective and cancer-curative effects with minimal damaging effects on normal cells. In particular, product **RE4** has the best ambush effect versus the drastic brands. Product **RE6** exhibited a potent cancer-curative activity compared with 5F-uracil and the other extracted coumarins with the best undamaging effect on normal cell line. Accordingly, the author proposed that product **RE4** could provide a valuable structural template for synthesizing a potent oxidation-protective agent with significant safety. Furthermore, product **RE6** can serve as a foundation stone for the development of potent cancer-curing medications with minimal toxicity to normal tissue.

Acknowledgements

The authors are praising the University of Mosul/College of Pharmacy for providing facilities that improved the quality of this work. The authors would also like to thank Dr. Sarah Ahmed Waheed, Dr. Rahma Mowaffaq Jebir, and Dr. Sara Firas Jasim for their help regarding the literature search.

Orcid:
Reem Nadher Ismael:
https://www.orcid.org/0000-0002-4598-4782
Yasser Fakri Mustafa:
https://www.orcid.org/0000-0002-0926-7428
Harith Khalid Al-Qazaz:
https://www.orcid.org/0000-0002-5223-0065

References

[1] M.K. Oglah, Y.F. Mustafa, M.K. Bashir, M.H. Jasim, *Syst. Rev. Pharm.*, **2020**, *11*, 472–481. [Pdf], [Google Scholar], [Publisher]
[2] Y.F. Mustafa, *Saudi Pharm. J.*, **2018**, *26*, 870–875. [Crossref] [Google Scholar] [Publisher]
[3] Y.F. Mustafa, R.R. Khalil, E.T. Mohammed, *Syst. Rev. Pharm.*, **2020**, *11*, 382–387. [Pdf], [Google Scholar], [Publisher]
[4] Y.F. Mustafa, *Appl. Nanosci.*, **2021**. [Publisher], [Google Scholar]
[5] J. Finaud, G. Lac, E. Filaire, *Sports Medicine*, **2006**, *36*, 327. [Crossref], [Google Scholar], [Publisher]
[6] Y.F. Mustafa, M.K. Bashir, M.K. Oglah, R.R. Khalil, E.T. Mohammed, *NeuroQuantology*, **2021**, *19*, 129–138 [Crossref], [Google Scholar], [Publisher]

[7] R.C. Fierascu, I. Fierascu, S.M. Avramescu, E. Sieniawska, *Molecules*, **2019**, *24*, 1–29. [Crossref], [Google Scholar], [Publisher]
[8] M.K. Oglah, Y.F. Mustafa, *J. Glob. Pharma Technol.*, **2020**, *12*, 854–862. [Pdf], [Google Scholar], [Publisher]
[9] R.A. Khan, *Saudi Pharm. J.*, **2018**, *26*, 739–753. [Crossref], [Google Scholar], [Publisher]
[10] Y.F. Mustafa, E.T. Mohammed, R.R. Khalil, *Syst. Rev. Pharm.*, **2020**, *11*, 570–576. [Pdf], [Google Scholar], [Publisher]
[11] H.S. Budi, M.F. Jameel, G. Widjaja, M.S. Alasady, T. Mahmudiono, Y.F. Mustafa, I. Fardeeva, M. Kuznetsova, *Braz. J. Biol.*, **2022**, *84*, 1-7. [Crossref], [Google Scholar], [Publisher]
[12] M.K. Bashir, Y.F. Mustafa, M.K. Oglah, *Period. Tche Quim.*, **2020**, *17*, 871–883. [Crossref], [Google Scholar], [Publisher]
[13] Y.F. Mustafa, *J. Glob. Pharma Technol.*, **2019**, *11*, 1–10. [Google Scholar], [Publisher]
[14] S.F. Jasim, Y.F. Mustafa, *Iraqi Journal of Pharmacy*, **2021**, *18*, 104-125. [Crossref], [Google Scholar], [Publisher]
[15] A.M. Nejres, Y.F. Mustafa, H.S. Aldewachi, *Int. J. Pavement Eng.*, **2022**, *23*, 39–45. [Crossref], [Google Scholar], [Publisher]
[16] Y.F. Mustafa, N.T. Abdulaziz, *NeuroQuantology*, **2021**, *19*, 175–186. [Crossref], [Google Scholar], [Publisher]
[17] Y.F. Mustafa, S.M. Kasim, B.M. Al-Dabbagh, W. Al-Shakarchi, *Appl. Nanosci.*, **2021**. [Crossref], [Google Scholar], [Publisher]
[18] M.S. Majoumouo, N.R.S. Sibuyi, M.B. Tincho, M. Mbekou, F.F. Boyom, M. Meyer, *Int. J. Nanomedicine*, **2019**, *14*, 9031–9046. [Pdf], [Google Scholar], [Publisher]
[19] Y.F. Mustafa, E.T. Mohammed, R.R. Khalil, *Egypt. J. Chem.*, **2021**, *64*, 4461–4468. [Crossref], [Google Scholar], [Publisher]
[20] M. Umair, D. Kim, M. Choi, *Scientific Reports,* **2020**, *10*, 1–13. [Crossref], [Google Scholar], [Publisher]
[21] E.T. Mohammed, Y.F. Mustafa, *Syst. Rev. Pharm.*, **2020**, *11*, 64–70. [Pdf], [Google Scholar], [Publisher]
[22] N.I. Yusoff, C.P. Leo, *J. Food Qual.*, **2017**, 2017. [Crossref], Google Scholar], [Publisher]
[23] R.R. Khalil, Y.F. Mustafa, *Syst. Rev. Pharm.*, **2020**, *11*, 57–63. [Pdf], [Google Scholar], [Publisher]
[24] Y.F. Mustafa, M.K. Bashir, M.K. Oglah, *Syst. Rev. Pharm.*, **2020**, *11*, 598–612. [Crossref], [Google Scholar], [Publisher]
[25] S.H. Haq, G. Al-Ruwaished, M.A. Al-Mutlaq, S.A. Naji, M. Al-Mogren, S. Al-Rashed, Q.T. Ain, A.A. Al-Amro, A. Al-Mussallam, *Scientific reports.*, **2019**, *9*, 18906. [Crossref], [Google Scholar], [Publisher]
[26] A.B. Roomi, G. Widjaja, D. Savitri, A.T. Jalil, Y.F. Mustafa, L. Thangavelu, G. Kazhibayeva, W. Suksatan, S. Chupradit, S. Aravindhan, *J. Nanostructures*, **2021**, *11*, 514-523. [Crossref], [Google Scholar], [Publisher]
[27] Y.F. Mustafa, *NeuroQuantology*, **2021**, *19*, 99–112. [Crossref], [Google Scholar], [Publisher]
[28] M.K. Oglah, Y.F. Mustafa, *J. Med. Chem.*, **2020**, *29*, 479–486. [Crossref], [Google Scholar], [Publisher]
[29] H. Aldewachi, Y.F. Mustafa, R. Najm, F. Ammar, *Syst. Rev. Pharm.*, **2020**, *11*, 289–296. [Pdf], [Google Scholar], [Publisher]
[30] Y.F. Mustafa, N.A. Mohammed, *Biochem. Cell. Arch.*, **2021**, *21*, 1991–1999. [Google Scholar], [Publisher]
[31] Y.F. Mustafa, N.T. Abdulaziz, *Syst. Rev. Pharm.*, **2020**, *11*, 438–452. [Pdf], [Google Scholar], [Publisher]
[32] Y.F. Mustafa, M.K. Oglah, M.K. Bashir, E.T. Mohammed, R.R. Khalil, *Clin. Schizophr. Relat. Psychoses,* **2021**, *15*, 1–6. [Crossref], [Google Scholar], [Publisher]
[33] C.N. Teijaro, A. Adhikari, B. Shen, *J. Ind. Microbiol. Biotechnol.*, **2019**, *46*, 433–444. [Crossref], [Google Scholar], [Publisher]
[34] Y.F. Mustafa, M.K. Oglah, M.K. Bashir, *Syst. Rev. Pharm.*, **2020**, *11*, 482–489. [Google Scholar], [Publisher]
[35] S.L. Robinson, J.K. Christenson, L.P. Wackett, *Nat. Prod. Rep.*, **2019**, *36*, 458–475. [Crossref], [Google Scholar], [Publisher]

[36] M.K. Bashir, Y.F. Mustafa, M.K. Oglah, *Syst. Rev. Pharm.*, **2020**, *11*, 175–187. [Pdf], [Google Scholar], [Publisher]
[37] J. Widelski, S.V. Luca, A. Skiba, I. Chinou, L. Marcourt, J.L. Wolfender, K. Skalicka-Wozniak, *Molecules*, **2018**, *23*. [Crossref], Google Scholar], Publisher]
[38] M.K. Oglah, M. Kahtan Bashir, Y. Fakri Mustafa, E.T. Mohammed, R.R. Khalil, *Syst. Rev. Pharm.*, **2020**, *11*, 717–725. [Pdf], [Google Scholar], [Publisher]
[39] G. Borges Bubols, D. da Rocha Vianna, A. Medina-Remon, G. von Poser, R. Maria Lamuela-Raventos, V. Lucia Eifler-Lima, S. Cristina Garcia, *Mini Rev. Med. Chem.*, **2013**, *13*, 318–334. [Crossref], [Google Scholar], [Publisher]
[40] M. Javed, A. Saade, A. Jasim, T. Zeedan, T. Dmitry, O. Bokov, Mohammed Nader Shalaby, Moaed E. Al-Gazally, Hamzah H. Kzar, M.T. Qasim, Y.F. Mustafa, M. Khatami, *J. Clust. Sci.*, **2022**, *4*, 44–47. [Crossref], [Google Scholar], [Publisher]

How to cite this article: Reem Nadher Ismael*, Yasser Fakri Mustafa, Harith Khalid Al-Qazaz. Cancer-curative potential of novel coumarins from watermelon princess: A scenario of their isolation and activity. *Eurasian Chemical Communications*, 2022, 4(7), 657-672. Link: http://www.echemcom.com/article_147420.html